Time-resolved Analysis of Primary Volatile Emissions and Secondary Aerosol Formation Potential from a Small-Scale Pellet Boiler

Hendryk Czech[a], *Simone M. Pieber*[b], *Petri Tiitta*[c], *Olli Sippula*[c,d], *Miika Kortelainen*[c], *Heikki Lamberg*[c], *Julija Grigonyte*[c], *Thorsten Streibel*[a,d,e,*], *André S. H. Prévôt*[b], *Jorma Jokiniemi*[c,d], *Ralf Zimmermann*[a,d,e]

[a]Joint Mass Spectrometry Centre, Chair of Analytical Chemistry, Institute of Chemistry, University of Rostock, 18059 Rostock, Germany

[b]Laboratory of Atmospheric Chemistry, Paul Scherrer Institute, CH-5232, Villigen, Switzerland

[c]Fine Particle and Aerosol Technology Laboratory, Department of Environmental and Biological Sciences, University of Eastern Finland, FIN-70211 Kuopio, Finland

[d]Helmholtz Virtual Institute of Complex Molecular Systems in Environmental Health (HICE) - www.hice-vi.eu

[e]Joint Mass Spectrometry Centre, Cooperation Group "Comprehensive Molecular Analytics" (CMA), Helmholtz Zentrum München – German Research Centre for Environmental Health, 85764 Neuherberg, Germany

*corresponding author;

phone: +49 381 498 6536, fax: +49 381 498 118 6527, email: thorsten.streibel@uni-rostock.de

Keywords: VOC, photoionization, SP-AMS, PAM flow reactor, wood combustion, SOA

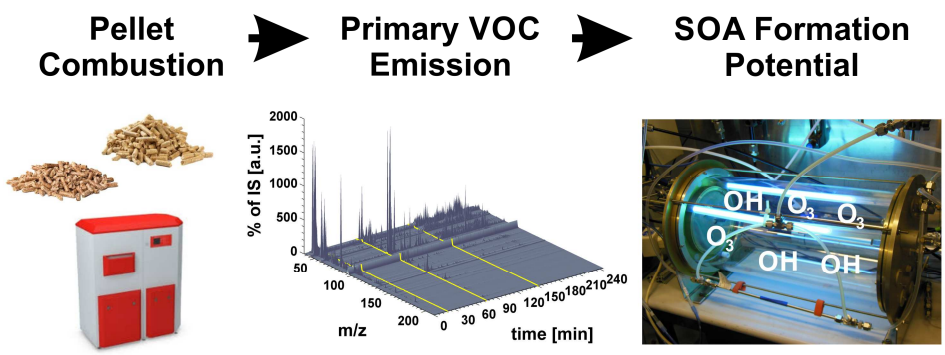

Abstract

Small-scale pellet boilers and stoves became popular as a wood combustion appliance for domestic heating in Europe, North America and Asia due to economic and environmental aspects. Therefore, an increasing contribution of pellet boilers to air pollution is expected despite their general high combustion efficiency. As emissions of primary organic aerosol (POA) and permanent gases of pellet boilers are well investigated, the scope of this study was to investigate the volatile organic emissions and the formation potential of secondary aerosols for this type of appliance. Fresh and aged emissions were analysed by a soot-particle aerosol time-of-flight mass spectrometry (SP-AMS) and the molecular composition of the volatile precursors with single-photon ionisation time-of-flight mass spectrometry (SPI-TOFMS) at different pellet boiler operation conditions. Organic emissions in the gas phase were dominated by unsaturated hydrocarbons while wood-specific VOCs, e.g. phenolic species or substituted furans, were only detected during the starting phase. Furthermore, organic emissions in the gas phase were found to be correlated to fuel grade and combustion technology in terms of secondary air supply. Secondary organic aerosols of optimised pellet boiler conditions (OPT, state-of-the-art combustion appliance) and reduced secondary air supply (RSA, used as a proxy for pellet boilers of older type) were studied by simulating atmospheric ageing in a Potential Aerosol Mass (PAM) flow reactor. Different increases in OA mass (55 % for OPT, 102 % for RSA), associated with higher average carbon oxidation state and O:C, could be observed in a PAM chamber experiment. Finally, it was found that derived SOA yields and emission factors were distinctly lower than reported for log wood stoves.

1. Introduction

Since the mid-nineties, the demand in Europe for wood pellets as a fuel for domestic heating grows steadily due to high fossil fuel prices, fuel taxes, incentives for renewable energy and CO_2-balance (Cocchi, 2011; Madlener and Koller, 2007). In 2010, the pellet consumption in the European Union (EU27) accounted for 9.8 mio tons (Audigane et al., 2012) while an expanding market is expected for Europe, North America and Asia (Cocchi, 2011). Wood pellets can be utilised in stoves or boilers, whereby boilers are preferred in Northern and Central Europe. From 2005 to 2010, in Germany as the main European market between 15,000 and 25,000 small-scale boilers (power < 50 kW) were newly installed every year (Audigane et al., 2012). Domestic biomass burning is known to emit large amounts of several air pollutants, such as particulate matter (PM), black carbon (BC), particle-bound organic matter (OM), volatile organic compounds (VOCs), carbon monoxide and NO_x (Eriksson et al., 2014; Evtyugina et al., 2014; Heringa et al., 2012; Kinsey et al., 2012; Martinsson et al., 2015; Orasche et al., 2012; Stockwell et al., 2014), but in many studies, continuously-fired pellet boilers have been characterised as low-emitting combustion appliances compared to batchwise combustion of wood fuels in modern or conventional log wood stoves (Lamberg et al., 2011a; Obaidullah et al., 2012; Orasche et al., 2012; Ozgen et al., 2014; Reda et al., 2015). However, the raw material for pelletisation and the operating conditions in terms of load have been found to affect the emissions (Chandrasekaran et al., 2013; Heringa et al., 2012; Sippula et al., 2007; Venturini et al., 2015; Verma et al., 2011; Vicente et al., 2015; Win et al., 2012). Additionally, particle emissions from pellet boilers and stoves are considerably higher compared to small-scale oil boilers as an alternative with fossil fuel in single-house heating systems (Kaivosoja et al., 2013).

Emission of organic vapours are often expressed as cumulative quantities, e.g. total hydrocarbons (THC), non-methane hydrocarbons/volatile organic compounds (NMHC/NMVOC) or organic gaseous carbon (OGC), but only few studies have paid attention to the investigation of the molecular composition of VOCs released from pellet boilers (Aurell et al., 2012; Boman et al., 2011; Johansson et al., 2004; Olsson et al., 2003; Sippula et al., 2007).

Among the severe effect on human health by wood combustion aerosol (Jalava et al., 2012; Miljevic et al., 2010; Mülhopt et al., 2016; Sehlstedt et al., 2010), VOC emissions from wood combustion contribute to ambient particle concentrations as secondary organic aerosol (SOA) through gas-to-particle conversion (Hennigan et al., 2011; Heringa et al., 2011; Huang et al., 2015; Keller and Burtscher, 2012). In the atmosphere VOCs are transformed by photolysis, hydroxyl (OH) radicals (typically during daylight hours), nitrate radicals (NO_3) during evening and night-time hours, ozone (O_3), and in coastal and marine areas by chlorine atoms during daylight hours (Atkinson and Arey, 2003). The formed SOA may feature

different effects of human health (Künzi et al., 2013; Nordin et al., 2015) and affect the climate through its higher hygroscopicity and impact on cloud formation compared to the primary organic aerosol (POA) (Trivitayanurak and Adams, 2014). Recently, it has been found that the SOA formation from log wood combustion emissions is strongly dominated only by few compounds (Bruns et al., 2016), which mainly belong to the group of aromatic and functionalised aromatic hydrocarbons. Therefore, high concentrations of VOCs do not have to be related to high SOA formation potential and vice versa. To the best of our knowledge, only few studies have investigated the SOA formation from small-scale pellet stoves, but of the same manufacturer, by using a smog chamber or micro smog chamber flow reactor to generate SOA and a high-resolution aerosol mass spectrometer (Corbin et al., 2015; Heringa et al., 2011; Keller and Burtscher, 2012). In addition to that, the easing effect of pellet boiler emissions on SOA formation from α-pinene was recently described (Kari et al., 2017).

The scope of this study is to give a more detailed view over the organic emissions in the gas phase, to extend the database of emission factors (EFs) of volatile organic compounds (VOC) under different operating conditions for a combustion appliance becoming steadily more common and to evaluate its SOA formation.

2. Experimental

2.1. Combustion appliance and procedure

The combustion experiments were performed with an automatically-fired 25 kW top-feed pellet boiler (PZ25RL, Biotech Energietechnik GmbH, Austria), which is equipped with staged combustion secondary air feed. A detailed description of the combustion appliances can be found elsewhere (Lamberg et al., 2011b). Emissions of the pellet boiler were analysed at different operating conditions including boiler start phase (BSP, n = 7), optimal combustion (OPT, n = 7) and approximately 30 % reduced secondary air supply (RSA, n = 3). Since our combustion appliance is a state-of-the-art pellet boiler, RSA is regarded as a simulation of pellet boiler emissions of previous generations with less optimised combustion technology. The end of BSP was set to the point of time when EF of OGC undercuts the mean EF of OGC for OPT plus three-fold standard deviation. All combustion conditions were carried out with commercially available softwood pellets (Table 1). Additionally, the optimal combustion emissions were investigated with birch bark pellets (BBP, n = 1). In contrast to pellet stoves, which refer to room heating appliances, pellet boilers are usually connected to a reservoir of water for warm water supply, leading to a more continuous operation mode of the boiler rather than start-stop operation.

Table 1

Elemental composition and properties of the wood pellets.

	unit[a]	LOQ[b]	method	softwood pellets	birch bark pellets

water	m-%	0.1	DIN EN 14774-2	7.3	4.3
ash content 550°C	m-%	0.1	DIN EN 14775	0.36	1.6
carbon	m-%	0.2	DIN EN 15104	51.7	60.9
hydrogen	m-%	0.1	DIN EN 15104	6.0	7.1
nitrogen	m-%	0.05	DIN EN 15104	0.29	0.65
oxygen	m-%	-	calculated	41.6	29.8
sulphur	m-%	0.005	DIN EN 15289	0.006	0.023
chlorine	m-%	0.005	DIN EN 15289	0.006	0.018
lower heating value	kJ/kg	200	DIN EN 14918	19680	25360

[a] *related to dry matter*

[b] *limit of quantification*

2.2. Instrumentation

2.2.1. Gas measurements

Main components of the flue gas including carbon monoxide (CO), carbon dioxide (CO_2), oxygen (O_2) and nitrogen oxides (NO_x = NO+NO_2) were measured continuously by a gas analyser system (ABB, Limas 11 UV, Switzerland) at 2 s time resolution. The sum emissions of organic gaseous carbon (OGC) were quantified by a flame ionisation detector (ABB, Multi-FID 14, Switzerland), which was calibrated against propane. Water and methane were analysed by Fourier-transformed infrared spectroscopy (FTIR) gas analyser (Gasmet, Finland). All gaseous emissions were measured directly from undiluted stack gas through an insulated and externally heated sampling line at 180 °C.

2.2.2. Single photon ionisation time-of-flight mass spectrometry (SPI-TOFMS) for VOC analysis

VOCs were analysed by a time-of-flight mass spectrometer (TOFMS; *Compact Reflectron Time-of-Flight Spectrometer II,* Kaesdorf Geräte für Forschung and Industrie, Germany) with single-photon ionisation (SPI) at 118 nm (photon energy of 10.49 eV). A detailed description of the instrumental setup can be found elsewhere (Czech et al., 2016). In brief, undiluted hot flue gas was filtered and sampled at 220°C with stepwise increasing temperature to 245°C to prevent condensation. Entering the ionisation chamber of the mass spectrometer, flue gas components are hit by a laser beam (Nd:YAG, *Spitlight400*, Innolas GmbH, Germany) with a wavelength of 118 nm for single-photon ionisation (SPI). SPI refers to a soft ionisation technique, thus leading to predominantly molecular ions and low fragmentation. In principle, compounds with ionisation energies below the applied photon energy of 10.49 eV can be ionised (Hanley and Zimmermann, 2009). Finally, mass spectra were acquired at 20 Hz, averaged and stored with 1 s time resolution. During the combustion experiments, D_3-toluene (toluene (methyl-D_3), 98% purity, Cambridge Isotope Laboratories Inc., USA) was constantly added as internal standard (IS) leading to a concentration of 91 µl/m^3 (= 91 ppbv) in the raw gas. Semi-quantification of selected volatile species was based on photoionisation cross sections (PICS) relative to the IS of D_3-toluene (Table S1).

2.2.3. Soot-particle aerosol mass spectrometer (SP-AMS)

To analyse the organic fraction of primary and aged pellet boiler OA, a soot particle aerosol mass spectrometer (SP-AMS, Aerodyne Research Inc., USA) (Onasch et al., 2012) was applied with 100 % transmission for particles covering a vacuum-aerodynamic diameter from 75 nm to 650 nm (Liu et al., 2007). The SP-AMS is equipped with a continuous wave laser vaporiser at 1,064 nm based on single particle soot photometer technology (SP2, Droplet Measurement Technologies, CO, USA; (Stephens et al., 2003)) which enables in combination with the thermal vaporiser (600 °C) to study non-refractory as well as refractory, light absorbing particles such as refractive black carbon (rBC). Vaporised particle components were ionised by electron impact at 70 eV. Subsequently formed ions were separated in a high resolution time-of-flight mass spectrometer (HR-TOFMS) operated in V-mode from m/z 12 to m/z 555 at a mass resolution of approximately 2,000 at m/z 28. All presented data related to OA were recorded without laser vaporiser. AMS data analysis was performed with the analysis software SQUIRREL v1.55C and the standard HR-ToF-AMS data analysis software Peak Integration by Key Analysis (PIKA v1.16 C) adapted in Igor Pro 6.34 A (Wavemetrics). Determination of HR mass concentrations, elemental analysis and ratio of organic mass (OM) to organic carbon (OC) were performed using standard fragmentation assumptions (Allan et al., 2003; Jimenez et al., 2003), and the methods described by (Canagaratna et al., 2015) and (Aiken et al., 2008), respectively. A detailed description of the instrument performance, data analysis and calibration can be found in (Tiitta et al., 2016).

2.4. PAM flow reactor and ageing experiments

The PAM flow reactor in this study was firstly constructed by (Kang et al., 2007) and basically used in the version and settings described by (Bruns et al., 2015). PAM aims to investigate the maximum OA mass after oxidation of precursor gases, nucleation, condensation and gas-particle-partitioning within a short time period in contrast to real-time ageing in smog chambers. Therefore, elevated concentrations of OH compared to typical ambient levels are applied (Li et al., 2015). Briefly, the PAM comprises of a single glass cylinder of 0.015 m^3 (length: 0.46 m, diameter: 0.22 m), equipped with two UV-lamps (peak emission at 185 nm and 254 nm, BHK Inc.). In all ageing experiments, UV-lamps were operated at full power (110 V lamp voltage), generating ozone and OH radicals. Ozone is formed by photolysis of O_2 in to $O(^3P)$ which reacts with O_2 and a collision partner. From photolysis of ozone, $O(^1D)$ is formed and reacts with water to OH radicals (Ehhalt, 1999). To provide appropriate water for this reaction, 1 L min^{-1} of humidified pure nitrogen (“Nafion humidifier”, Perma Pure LLC) was added to the diluted exhaust (1:20 for both OPT and RSA by a porous tube dilutor) gas before entering the PAM to achieve a relative humidity between 21 % and 26 %. The sampling flow of 5 L min^{-1} for measuring instruments and a ring flow of 3 L min^{-1} result in a residence time of 112.5 s. SPI-TOFMS and SP-AMS sampled without additional dilution from

the PAM except SP-AMS measurements of RSA (additional dilution of 1:10 by ejector dilutor).

The initial concentrations of the ageing experiments with PAM flow reactor are summarised in Table 2. OH exposure to VOCs was determined by the degradation of toluene from the pellet boiler emission (Barmet et al., 2012), analysed by SPI-TOFMS, at a rate constant of $5.63 \cdot 10^{-12}$ cm^3 $molec^{-1}$ s^{-1} at 298 K (Atkinson and Arey, 2003). In contrast to (Barmet et al., 2012) who demonstrated their concept on a 2-stroke moped, the pellet boiler emissions feature a distinct lower ratio of VOCs (measured as OGC) to NO_x. Low calculated OH exposures may be a result of partly consumed O_3 in the oxidation of NO to NO_2 and consequently lower OH production rate or reaction of NO_2 with OH to HNO_3 (Tkacik et al., 2014).

One PAM cycle denotes one hour with UV light on and one hour with UV light off while during approximately the first 15 min of one cycle were waited to reach steady-state conditions. For OPT two cycles and for RSA one cycle were included in the data evaluation.

It has been reported that particle wall losses affect the measured SOA yield (Lambe et al., 2011), which accounted for 1 % to 33 % by mass in previous studies (Bruns et al., 2015; Ortega et al., 2013). It is expected that not more than 30 % of the particles are lost based on similar size distributions measured by SP-AMS (Fig. S1) with a transmission of > 80% for particles with a mobility diameter > 150 nm (Lambe et al., 2011) and a previous study with the same pellet boiler and similar soft wood pellets by Lamberg et al. (2011).

Although it has been recently shown that SOA coating of BC particles affect rBC results from SP-AMS (Ahern et al., 2016), rBC were regarded as stable because of low SOA formation. Increases in OA mass (OA enhancement ratios (ER_{OA})) when UV light was switched on were calculated after normalisation to rBC, which intrinsically includes the size-dependence of the particle wall losses in the size-range of AMS particle transmission.

$$ER_{OA} = (OA_{UV(on)} / rBC_{UV(on)}) / (OA_{UV(off)} / rBC_{UV(off)}) \quad (1)$$

The calculation is equal to the method described by (Grieshop et al., 2009) with replacing BC by rBC. $ER_{OA} > 1$ stands for a net increase in OA mass where as $ER_{OA} < 1$ mean a loss in OA mass. Concentrations of OGC inside the PAM were calculated from measurements before the PAM and the respective dilution ratio. In contrast to particles, losses of vapours are regarded as negligible due to the short residence time (Ortega et al., 2013).

An overview of the entire instrumental setup can be found in the supplementary material (Fig. S2).

Table 2

Initial concentrations for PAM flow reactor experiments with optimal pellet boiler settings (OPT) and reduced secondary air (RSA).

experiment	POA[a] (µg m^{-3})	CH_4 (µg m^{-3})	OGC (µg m^{-3})	POA/CO (µg m^{-3} ppm^{-1})	OH exposure[b] (10^6 molec cm^{-3} h)	MCE[c]
OPT	12	75.6	104	3.8	17.6	0.9993
RSA	132	10.8	68	17.8	-[d]	0.9964

[a] *lower limit due to unknown wall losses, approximately 29-33 % (Bruns et al., 2015)*

[b] *calculated from decay of toluene with UV on and off behind PAM*

[c] *modified combustion efficiency, calculated as $\Delta[CO_2] / (\Delta[CO_2]+\Delta[CO])$*

[d] *OH exposure not available because of malfunction in data acquisition*

3. Results & Discussion

3.1. Primary Emissions

3.1.1. Characterisation of organic vapours in flue gas under different pellet boiler operation conditions

All acquired mass spectra were sorted by operation condition and averaged (Fig. 1). Many of the observed m/z can be assigned to well-known pyrolysis gases from wood combustion, such as propene (m/z 42), acetaldehyde (m/z 44), butane/acrolein (m/z 56), acetone/propanal (m/z 58), benzene (m/z 78) and toluene (m/z 92). In the smaller mass region from m/z 40 to m/z 74, peaks appear in groups (triplets to multiplets) of even m/z over m/z intervals of 6-10. Assuming that the vast majority of the VOC in the emission comprises of carbon, oxygen and hydrogen, the number of possible sum formulae shrinks through meaningful number of double bond equivalents and chemical bonds, which allows postulating sum formulas without information of the exact mass. Peaks of the lowest m/z of those multiplets cannot have a chemically meaningful sum formula containing oxygen. Therefore, the mass spectra give evidence that polyunsaturated hydrocarbons, such as propadiene/propyne (m/z 40), vinylacetylene (m/z 52) or cyclopentadiene (m/z 66) are over-proportionately represented in pellet boiler emissions compared to less controlled wood combustion (Czech et al., 2016). The upper m/z of the multiplets likely appertain to carbonyl compounds, indicating a general low abundance of volatile oxygenates in the pellet boiler emission. Phenolic species from lignin (guaiacol m/z 124, methyl-guaiacol m/z 138, vanillin m/z 152) and furans from carbohydrate degradation (methyl-furan m/z 82, furfural m/z 96, furfuryl alcohol m/z 98) emerge with higher abundances from the BSP mass spectrum compared to other operation conditions. Thus primary decomposition of the wood biopolymers plays only an important role in the combustion during the starting phase of the boiler, where the highest abundances for any m/z could be observed, despite the higher PICS and associated sensitivity of SPI for aromatic species (Adam and Zimmermann, 2007). When the boiler operates with optimal conditions OPT, most m/z > 100 Th observed in BSP drop below the limit of detection. When the secondary air supply was reduced by 30 %, intensities of aromatic hydrocarbons, such as benzene (m/z 78) and naphthalene (m/z 128),

increased by one order of magnitude, whereas aliphatic polyunsaturated hydrocarbons, such as vinylacetylene (m/z 52) and butadiene (m/ 54), increased by 50 % and 300 %, respectively. However, oxygenates, such as acetaldehyde (m/z 44) and C3-carbonyls (m/z 58) remained constant compared to OPT. Hence, the RSA combustion scenario leads to the highest ratio of unspecified to biomass-related products of incomplete combustion, which may aggravates the assignment of pellet boiler emissions to wood combustion in source apportionment studies. The burning of low-grade wood pellets produced from birch bark results in comparable quantitative VOC emissions to RSA with high-quality softwood pellets regardless the optimal combustion conditions. Higher emissions of aromatics hydrocarbons compared to OPT (e.g. benzene, toluene, naphthalene) can be explained by the higher content of lignin (Krutul et al., 2011) and consequently higher content of aromatic (phenolic) species in the bark compared to the stem.

3.1.2. Modified combustion efficiency, concentrations and emission factors of gases and VOCs

Mean EFs in mg/MJ with standard deviation for repeated measurements were calculated according to the Finnish Standard Association method SFS 5624 as described by (Reda et al., 2015) and presented in Table 3. Additionally, median, 5th and 95th percentile of all data points under one condition can be found in Table S2 of the supplemental material, which describes the temporal appearing variances of the emission in a more appropriate manner.

The observed modified combustion efficiencies (MCE = $\Delta CO_2/(\Delta CO_2+\Delta CO)$) were found to be generally high (> 0.99) for all continuous operations OPT, RSA and BBP at full load, which emphasises the very efficient combustion. Analyte time traces of an experimental run covering all four operating conditions are illustrated in Fig. 2 to underline different types of temporal evolutions.

From BSP to OPT, CO_2 increased to (8.6±0.3) % and O_2 decayed to (11.9.0±0.3) % from ambient levels. EF of NO_x were found to have almost equal means in BSP and OPT, but different standard deviations (BSP: (63.8±7.4) mg/MJ); OPT: (63.5±2.9) mg/MJ). The reduced secondary air and associated reduced oxygen supply slightly declined NO_x-EF to (57.7±1.1) mg/MJ, whereas the birch bark pellet combustion under optimised conditions increased NO_x to 131.0 mg/MJ. Compared to softwood pellets birch bark pellets contain twice as much nitrogen (Table 1), indicating that NO_x emissions are mainly caused by fuel-nitrogen oxidation (Garcia-Maraver et al., 2014).

The progression of CO-EF was similar to EF of OGC: Both EFs peaked during BSP with mean EFs of (580.0±270.4) mg/MJ (CO) and (55.0±28.9) mg/MJ (OGC), but decreased rapidly to less than 1 % of the maximum EF within 2 min after start. During OPT, the pellet boiler emits very low amounts of OGC ((1.3±0.1) mg/MJ) and CO ((45.9±9.0) mg/MJ), respectively. Waiving full secondary air supply was found to increase CO

(382.3±93.8 mg/MJ) by almost one order of magnitude and OGC (2.9±0.6 mg/MJ) by a factor of two compared to OPT, which emphasises the benefit of this advanced combustion technology. Switching to low-grade birch bark pellets leads to a similar effect in terms of OGC (3.4 mg/MJ) and CO (180.9 mg/MJ).

Although both low-grade BBP and RSA enhance OGC-EF, increased levels of single organic vapours turned out differently. Compared to OPT, OGC increased at RSA by 120 %, but acetaldehyde as a representative for oxygenates remained almost constant, whereas the polyenes vinylacetylene and butadiene rose by 100 % and benzene even by one order of magnitude. For BBP, higher releases could be observed for benzene, toluene and styrene, which might be enhanced by the higher availability of substituted aromatics from higher lignin content of the birch bark pellets (Krutul et al., 2011) and formation through cracking of side chains, but also for butadiene.

Classing the applied pellet boiler with small-scale automatically-fed pellet boiler of previous studies, it can be summarised that emission factors of CO and volatile organics were at the lower end of the published range, whereas NO_x was located in the mid-range of literature EFs (Table S3), which is mainly caused by the lower nitrogen content of the pellets. Low ratios of VOCs to NO_x are regarded as an indicator for a low potential secondary aerosol formation by OH (Ervens et al., 2008). Under optimal operation the ratio of OGC to NO_x does not exceed 0.05 unless the secondary air is reduced which can temporarily increase OGC/NO_x up to a still low value of 1.5.

Table 3

Modified combustion efficiency, mean concentrations of O_2 and CO_2 (both in %) and EFs for organic gaseous carbon (OGC), CO, NO_x and selected VOCs (in mg/MJ) at four operating conditions.

	MCE	O_2	CO_2	CO	NO_x	OGC	PRP m/z 42	AA m/z 44	VA m/z 52	BTD m/z 54	BENZ m/z 78	TOL m/z 92	STYR m/z 104	IND m/z 116	NAP m/z 128	MNAP m/z 142
BSP	0.9008	14.64	5.98	580.02	63.78	55.03	6.284	18.933	1.396	2.255	3.434	0.836	0.283	0.137	0.297	0.047
OPT	0.9993	11.93	8.57	45.92	63.49	1.30	0.037	0.238	0.011	0.016	0.023	0.007	0.004	0.002	0.010	0.005
RSA	0.9928	11.73	8.62	382.27	57.74	2.91	0.055	0.297	0.035	0.031	0.215	0.018	0.011	0.005	0.070	0.009
BBP	0.9969	11.89	7.85	180.93	131.60	3.44	0.102	0.291	0.029	0.071	0.151	0.020	0.010	0.003	0.035	0.005

PRP – propene; AA – acetaldehyde; VA – vinylacetylene; BTD – butadiene; BENZ – benzene; TOL – toluene; STYR – styrene; IND – indene; NAP – naphthalene; MNAP – methylnaphthalene; EFs can be converted into mg/kg wood by using lower heating values of softwood and birch bark pellets from Table 1

3.2. Secondary formation potential from PAM flow reactor

Pellet boiler emission for OPT and RSA passed through the PAM with UV-lights switched on and off. Data points at steady-state conditions were examined for statistically significant differences of their arithmetic means by two-sample Student's t-test.

3.2.1. Secondary VOC species

Apart from carbonyls, intensities of all volatile species declined regardless the combustion condition. For OPT conditions the homologue series of C_2- to C_5-carbonyls (m/z 44 to m/z 86) increased significantly ($p < 1 \cdot 10^{-6}$) by a factor of six for acetaldehyde and a factor of two for C_3- to C_5-carbonyls compared to the primary emission (Fig. S3). Further secondary volatile species could not be detected by SPI-TOFMS due to too high ionisation energies, possible fragmentation or too low concentrations. A statement about the secondary volatile species for RSA cannot be made because of a malfunction in data acquisition.

3.2.2. OA enhancement ratios ER_{OA}

Oxidation and enhanced functionalisation of volatile precursors result in decreasing vapour pressures leading to condensation, secondary particle formation and SOA. OA can also increase by heterogeneous oxidation of particulate organic matter (aged POA) (Browne et al., 2015). Based on the available data, it cannot be differentiated between aged POA and SOA. However, it was found that heterogeneous reactions of OH do not play a significant role at observed low OH exposures (Cappa and Wilson, 2012).

OA gained 1.55-fold additional mass (ER_{OA}, $p = 0.162$) after photooxidation of pellet boiler emission under stable OPT conditions. Only Keller & Burtscher (2012) observed SOA formation for the stable burning condition of a pellet stove with a micro-smog chamber (MSC), whereas no SOA was observed by Corbin et al. (2015) with the same ageing apparatus. With a smog chamber (SC) SOA yields were only observed for the pellet burner starting phase which emits higher amounts of VOCs than the stable burning phase for which SOA formation appeared within the uncertainty of wall loss correction (Heringa et al., 2011). Two possible explanations can be given by the different types of ageing reactor and combustion appliances: The MSC features shorter residence times, which can favour photo-fragmentation reaction and avoid particle coagulation (Bruns et al., 2015), leading to lower increases of OA and explaining the absence of SOA in the experiment of Corbin et al. (2015). Furthermore, the different type of combustion appliances likely play the major role for explaining the different SOA formation between Keller & Burtscher (2012) and Corbin et al. (2015) as well as between this study and Heringa et al. (2011) because it has been shown that PAM and SC generate comparable increases of OA exposing POA to the same total level of OH (Bruns et al., 2015). The gained relative weight in OM may suggest distinct SOA formation, but the initial POA concentration was low compared to organic compounds in the gas phase (Table 2), which might be the reason for the insignificance of OA increase.

Despite low concentrations of OGC during OPT, many (poly)unsaturated aliphatic hydrocarbons were detected in the primary emission which generally exhibit a high reactivity under OH and O_3 towards formation of highly functionalised SOA compounds (Ng et al., 2006). Due to the decreased vapour pressure even highly functionalised SOA components with a relatively low carbon number can condense on particles or form condensation nuclei.

On that account, it is likely that the high number of double bond equivalents of the primary emitted organic compounds induce higher gas-to-particle conversion rates than other organic vapours of lower double bond equivalent numbers.

Photooxidation of RSA pellet boiler emissions led to a higher growth in OA than photooxidation of OPT emissions with an ER_{OA} of 2.02 ($p = 2.8 \cdot 10^{-4}$). The reduction of secondary air by 30 % enhances POA mass by a factor of ~5, which agrees with the findings of (Lamberg et al., 2011b), whereas OGC in this study increased only by a factor of ~1.5 (Table 3). Similar to the higher ER_{OA}, RSA revealed higher SOA formation on an absolute scale, where the increase in OA is even one order of magnitude higher for RSA than OPT.

It might be that the relatively low OH exposure of $17.6 \cdot 10^6$ molec cm^{-3} h did not cover the full SOA formation potential. Towards higher relative humidity as used in other ageing studies of wood combustion emissions, the OH concentration were found to increase exponentially (Bruns et al., 2015), thus the observed ER_{OA} and related quantities represent lower limits.

3.2.3. Elemental ratios, average carbon oxidation state (OSC) and OM/OC

Under both operation conditions OPT and RSA, POA covered similar O:C of 1.07±0.41 (OPT) and 1.12±0.24 (RSA), which increased to 1.78±0.09 (OPT) and 1.37±0.24 (RSA) after photooxidation. Both O:C for POA and aged OA are higher than previously reported ratio 0.23 and 0.5 for stable burning (Heringa et al., 2011), but for POA a wide range of O:C for different pellet boiler makes up to 1.59 can be found for a 15 kW pellet boiler during stable combustion (Heringa et al., 2012). One reason for higher O:C compared to previous studies lies in the application of improved elemental analysis of AMS data which may enhance calculated O:C by 27 % related to the previous algorithm (Canagaratna et al., 2015). Additionally, high amounts of carbonates were found in pellet boiler particulate emissions (Lamberg et al., 2011a), which also might contribute to the CO_2^+ signal in the AMS spectra and enhance O:C (Bozetti et al., 2017). Nevertheless the increase of O:C is not affected since it is not known that photooxidation has an direct impact on the carbonate content. Recently, it has been demonstrated that KNO_3 have a positive bias on the CO_2^+ signal through reaction on the vaporiser and consequently increases O:C as well (Pieber et al., 2016). However, the impact of KNO_3 cannot be estimated because the AMS do not give quantitative data on potassium which inhibits the unambiguous assignment of NO_3^- to NH_4NO_3, organic nitrates and KNO_3. The ratio H:C behaved inversely to O:C and declined from 1.21±0.2 (OPT) and 1.31±0.15 (RSA) to 0.88±0.05 (OPT) and 1.20±0.15 (RSA). The relatively high degree of scattering for non-aged POA of OPT may be a consequence of low concentrations which implies higher errors for elemental analysis. Similar to previous studies (Corbin et al., 2015; Heringa et al., 2011), both POA and aged OA is located outside the triangular space where usually ambient aerosols can be found (Ng et al., 2010), which is possibly caused by faster gas-phase oxidation relative to particle nucleation (Lambe et al.,

2011).The average carbon oxidation state **(**OSC) (Kroll et al., 2011) increased accordingly to O:C from 0.88±0.94 (OPT) and 0.93±0.55 (RSA) to 2.68±0.23 (OPT) and 1.55±0.6 (RSA) (Fig. 3).

Taking into consideration that apart from carbonyls all m/z appeared with lower abundances in the SPI mass spectra with UV-lights on, gas-to-particle conversion was more likely the main mechanism for increasing OA mass than heterogeneous oxidation. The OM/OC ratios were elevated from 2.39±0.78 (OPT) and 2.60±0.31 (RSA) to 3.44±0.12 (OPT) and 2.93±0.31 (RSA). Moreover, the slope of H:C vs. O:C of aged OA provides information about oxidation mechanisms. Slopes of -0.44±0.07 (OPT) and -0.47±0.10 (RSA) were slightly higher than for aged wood burning aerosol (Ortega et al., 2013), but revealed that the addition of carboxylic groups associated with C-C bond breakage was the dominating mechanism (Ng et al., 2011) (Table S4).

3.2.4. High resolution mass spectrometric analysis of pellet boiler PM

The high resolution of the SP-AMS enables separation of isobaric ions and subsequent sorting into classes. Oxygenated species CHO_1 and $CHO_{n>1}$ dominated mass spectra of POA with 11 % and 53 % while CH represented 6 % in particles of OPT. For RSA, POA contained similarly high fractions of $CHO_{n>1}$ (47 %) and more of CH (22 %) and CHO (18 %) compared to OPT. CH species decayed during ageing covered by increasing fractions of oxygen- and nitrogen-containing species as expected. However, while $CHO_{n>1}$ (for OPT and RSA) and CHO (for OPT) remained almost constant during ageing, aged OA from RSA emissions contained a significantly larger fraction of single-oxidised species CHO than non-aged POA (Fig. 4). Furthermore, the remaining organic fraction (total organic reduced by CH, CHO and $CHO_{n>1}$) of most likely CHN and CHNO species (= CHN(O)) were elevated from 4 % to 13 % for RSA and from 26 % to 29 % for OPT, indicating the formation of nitrogen-containing organic compounds such as peroxyacyl nitrates or nitro compounds.

In a detailed view at single ions (Fig. S4), significant increases for RSA of not less than 100 % were observed for $C_2H_3O^+$ (m/z 43), CO_2^+ (m/z 44) and $C_2H_4O_2^+$ (m/z 60) which belong to typical SOA compound classes of non-acid oxygenates, carboxylic acids and long-chain carboxylic acids (Ng et al., 2011). In particular, the fragment $C_2H_4O_2^+$ (m/z 60) has been extensively discussed in the literature due to its application as marker for biomass burning, but also contributions from both SOA components and anhydrous sugars, such as levoglucosan, mannosan and galactosan (Elsasser et al., 2012; Heringa et al., 2011). The pure hydrocarbon fragments $C_3H_7^+$ (m/z 43) and $C_4H_9^+$ (m/z 57) decreased by 34 % and 44 % for RSA, respectively. Interestingly, the aromatic-related fragment $C_6H_5^+$ (m/z 77) significantly declined by 43 % ($p = 0.020$) for RSA, but increased by 77 % for OPT albeit insignificantly ($p = 0.084$). Taking the higher ratio of VOCs to POA for OPT into consideration, a transfer of oxygenated aromatics from the gaseous phase to the particulate

phase could have caused increasing $C_6H_5^+$ fragments. During ageing aromatic rings can only be retained by oxidation of side chains of substituted single-ring aromatics or PAHs. For example, the oxidation of toluene or naphthalene yields in benzaldehyde and phthalic acid, respectively (Riva et al., 2015; Wu et al., 2014). As opposed to RSA, OPT did not reveal any significant ($p < 0.05$) increase for any fragment ion except $C_2H_3O^+$ (m/z 43) by 510 % ($p = 6.16 \cdot 10^{-4}$) (Table S5).

3.2.5. Secondary organic carbon bulk yield (SOC_{yield}) and SOA formation potential

To calculate bulk yield of secondary organic carbon (SOC_{yield}), non-aged POA concentration was subtracted from aged OA concentration to obtain SOA resulting from gas-to-particle conversion. The known ratio of OM to OC was further incorporated to calculate the concentration of secondary SOC. Finally, SOC was set in relation to OGC, reduced by methane to non-methane organic gaseous carbon (NMOGC) (Table 2), assuming an equal FID response factor for both propane and methane, to reveal the relative amount of OGC which was transferred from gaseous into the particulate phase. For the SOC yield we assume that all NMOGC reacted despite the for PAM chamber relatively low OH exposure.

$$SOC_{yield} = (OA_{aged} - POA) / ((OM/OC)_{aged} \cdot NMOGC) \cdot 100\ \% \qquad (2)$$

While for RSA the conversion from OGC to SOC was 39.5 %, for OPT 4.1 % of NMOGC reacted with atmospheric oxidising agents to products of lower volatility which condense in the particulate phase. Thus, modern small-scale pellet boilers do not only emit low amounts of OA, but also account for a low contribution to the total particle level in ambient air after atmospheric conversion processes.

An estimation of SOA formation potential for BSP and BBP can be done by consideration of most contributing species to SOA formation (indicated by asterisk). Multiplication of *i* EFs of primarily emitted species, in this case of benzene, toluene, indene, naphthalene and methyl-naphthalene (Table 3), with their respective SOA yields (Bruns et al., 2016)

$$SOA^*\text{-}EF = \Sigma\ EF_i \cdot SOA_{yield,i} \qquad (3)$$

leads to SOA* potentials of 1661 µg/MJ (BSP), 17 µg/MJ (OPT), 108 µg/MJ (RSA) and 80 µg/MJ (BBP). Similar to (Heringa et al., 2011) the start phase BSP was found to emit higher levels of SOA precursors than the stable combustion phase OPT. However, ER_{OA}* of all combustion conditions appear in the small window of 1.33 to 1.36 and are lower than the obtained ER_{OA} from PAM experiments. The six considered organic species represent only a snapshot of organic vapours with significant SOA formation potential.

Comparing SOA-EFs and SOA*-EFs, the consideration of the six precursor leads only to one third of observed SOA formation from PAM experiments for OPT, while for RSA SOA-EFs is even one order of magnitude higher than SOA* indicating that distinctly more than the six considered precursors have a significant impact on SOA formation. In particular, oxygenated

monoaromatics, including phenol, methoxy-phenol or benzaldehyde, feature high SOA yields and may contribute significantly even at low concentrations. Moreover, some components e.g. acenaphthylene (m/z 152) or phenylacetylene (m/z 102), may contribute to the same extent as styrene to SOA formation (Bruns et al., 2016), but could not be quantified and thus may account for the observed discrepancy.

The SOA obtained by the combustion of the same amount of wood differs by one order of magnitude for this study compared to Keller & Burtscher (2012) for optimal as well as for reduced air conditions (Table 4), but their pellet stove was not equipped with air staged secondary air supply. Furthermore, both observed and calculated SOA mass per MJ during OPT are two orders of magnitude below the mean EF of 5±5.5 mg/MJ reported for the flaming phase of modern log wood stoves and three orders of magnitude lower than old wood stoves (Heringa et al., 2011). However, it should be kept in mind that EFs for batchwise log wood combustion and consequently the SOA formation potential, which is often reported solely for the first batch, may change enormously with ongoing batches when the temperature of the stove's combustion zone increases (Czech et al., 2016). Nevertheless, regarding these four combustion appliances, it is concluded that with improved combustion conditions not only the emission of VOCs is reduced, but also the SOA formation is suppressed.

Table 4

Emission factors of SOA from PAM experiments, (*)derived from sum of SOA yields of single precursors and literature data in mg/MJ with standard deviation in brackets

combustion condition	This study	This study*	Heringa et al. 2011[a]	Keller & Burtscher 2012[b]
BSP	-	1.661 (1.811)	28.5 (11.4)	-
OPT	0.053	0.017 (0.004)	0	0.394 (0.092)
RSA	1.150	0.108 (0.022)	-	12.22 (0.39); 51.46 (0.37); 325.83 (6.19)
BBP	-	0.080	-	-

based on SOA yields at OH exposures from 45 to 55·10^6 molec cm^{-3} h of benzene, toluene, styrene, indene, naphthalene and methyl-naphthalenes (Bruns et al., 2016) with an uncertainty of ±50 %; propagation error in brackets

[a] *converted from g/kg assuming a lower heating value of 20 MJ/kg*

[b] *converted from mg/kg-CO_2 assuming carbon content of 0.5 and lower heating value of 20 MJ/kg, three different settings of reduced air supply*

4. Conclusion

Primary and aged organic aerosol as well as VOCs from a small-scale pellet boiler were investigated by SP-HR-AMS and SPI-TOFMS. During continuous operation OPT, RSA and BBP, the pellet boiler emits one order of magnitude less VOCs, which mainly belong to the class of (poly)unsaturated hydrocarbons, compared to modern masonry heated burning logwood. Only in BSP and to a lower extend in BBP, typical wood combustion-related VOCs from the decomposition of carbohydrates and lignin, such as substituted furans and phenols, could be detected, which might bias apportionment to emission sources from measurements of ambient air.

In experiments with the PAM flow reactor, ER_{OA} of 1.55 and 2.02 were found for aged OA of OPT and RSA, respectively, which emphasises the relevance of organic vapours to total OA emission in ambient air not only for log wood stoves, but also for pellet boilers. Furthermore, the SOA formation potential was found to decrease with improvements of combustion technology from old log wood stoves (Heringa et al., 2011) to pellet boilers with air-staged secondary air supply by three orders of magnitude. However, a higher number of replicates has to support the evidence from these ageing experiments.

The fragment $C_2H_4O_2^+$ (m/z 60) represents the contribution of anhydrous sugars, mainly levoglucosan, to the mass spectrum of POA. In agreement with the findings of Heringa et al. (2011), a growth for this fragment was observed after ageing which expresses the contribution of pellet boiler SOA to the overestimation of primary biomass combustion emission in source apportionment studies derived from this fragment.

Altogether, our results demonstrate that VOC emissions from pellet boilers, as a growing combustion technology for domestic heating, cannot be regarded as typical wood combustion emission. Low emissions of VOCs are connected with low secondary aerosol formation potential compared to modern log wood stoves, which emphasises the role of pellet boilers as clean wood combustion appliances. Finally, this investigation also motivates to look closer into the change of the chemical composition of fresh aged particles from wood pellet combustion which is important in context with potential health effects associated with primary and aged emissions.

Acknowledgement

The measurements were carried out at the University of Eastern Finland (UEF), Department of Environmental and Biological Science, in cooperation with the Helmholtz Virtual Institute of Complex Molecular Systems in Environmental Health (HICE), funded by The Helmholtz Impulse and networking Funds of the Helmholtz Association (Germany), the DACH-project WooShi (grant ZI 764/5-1), the Academy of Finland (grants 259946, 258315 and 304459) and the University of Eastern Finland for the project ‘‘sustainable bioenergy, climate change and health”. Furthermore, Felix Klein is gratefully acknowledged for his valuable comments on the calculations.

References

Adam, T., Zimmermann, R., 2007. Determination of single photon ionization cross sections for quantitative analysis of complex organic mixtures. Analytical and Bioanalytical Chemistry 389, 1941-1951.

Ahern, A.T., Subramanian, R., Saliba, G., Lipsky, E.M., Donahue, N.M., Sullivan, R.C., 2016. Effect of secondary organic aerosol coating thickness on the real-time detection and characterization of

biomass-burning soot by two particle mass spectrometers. Atmospheric Measurement Techniques 9, 6117-6137.

Aiken, A.C., Decarlo, P.F., Kroll, J.H., Worsnop, D.R., Huffman, J.A., Docherty, K.S., Ulbrich, I.M., Mohr, C., Kimmel, J.R., Sueper, D., Sun, Y., Zhang, Q., Trimborn, A., Northway, M., Ziemann, P.J., Canagaratna, M.R., Onasch, T.B., Alfarra, M.R., Prevot, A.S.H., Dommen, J., Duplissy, J., Metzger, A., Baltensperger, U., Jimenez, J.L., 2008. O/C and OM/OC ratios of primary, secondary, and ambient organic aerosols with high-resolution time-of-flight aerosol mass spectrometry. Environmental Science and Technology 42, 4478-4485.

Allan, J.D., Jimenez, J.L., Williams, P.I., Alfarra, M.R., Jayne, J.T., Coe, H., Worsnop, D.R., 2003. Quantitative sampling using an Aerodyne aerosol mass spectrometer 1. Techniques of data interpretation and error analysis. Journal of Geophysical Research D: Atmospheres 108, AAC 1-1 - AAC 1-10.

Atkinson, R., Arey, J., 2003. Atmospheric Degradation of Volatile Organic Compounds. Chemical Reviews 103, 4605-4638.

Audigane, N., Bentele, M., Ferreira, J.M.F., Gyurik, A., Jossart, J.-M., Mangel, A.-C., Martin, M., Masdemont, P.R., Mörner, H., Paniz, A., Peieret, N., Rechberger, P., Rakos, C., Schlagitweit, C., Sievers, A.K., Tuohiniitty, H., 2012. European Pellet Report - PellCert Project 2012.

Aurell, J., Gullett, B.K., Tabor, D., Touati, A., Oudejans, L., 2012. Semivolatile and volatile organic compound emissions from wood-fired hydronic heaters. Environmental Science and Technology 46, 7898-7904.

Barmet, P., Dommen, J., DeCarlo, P.F., Tritscher, T., Praplan, A.P., Platt, S.M., Prévôt, A.S.H., Donahue, N.M., Baltensperger, U., 2012. OH clock determination by proton transfer reaction mass spectrometry at an environmental chamber. Atmospheric Measurement Techniques 5, 647-656.

Boman, C., Pettersson, E., Westerholm, R., Boström, D., Nordin, A., 2011. Stove performance and emission characteristics in residential wood log and pellet combustion, part 1: Pellet stoves. Energy and Fuels 25, 307-314.

Bozetti, C., et al., 2017. *manuscript in preparation*.

Browne, E.C., Franklin, J.P., Canagaratna, M.R., Massoli, P., Kirchstetter, T.W., Worsnop, D.R., Wilson, K.R., Kroll, J.H., 2015. Changes to the chemical composition of soot from heterogeneous oxidation reactions. Journal of Physical Chemistry A 119, 1154-1163.

Bruns, E.A., El Haddad, I., Keller, A., Klein, F., Kumar, N.K., Pieber, S.M., Corbin, J.C., Slowik, J.G., Brune, W.H., Baltensperger, U., Prévôt, A.S.H., 2015. Inter-comparison of laboratory smog chamber and flow reactor systems on organic aerosol yield and composition. Atmospheric Measurement Techniques 8, 2315-2332.

574 Bruns, E.A., El Haddad, I., Slowik, J.G., Kilic, D., Klein, F., Baltensperger, U., Prévôt, A.S.H., 2016.
575 Identification of significant precursor gases of secondary organic aerosols from residential wood
576 combustion. Scientific Reports 6, 27881.
577 Canagaratna, M.R., Jimenez, J.L., Kroll, J.H., Chen, Q., Kessler, S.H., Massoli, P., Hildebrandt Ruiz, L.,
578 Fortner, E., Williams, L.R., Wilson, K.R., Surratt, J.D., Donahue, N.M., Jayne, J.T., Worsnop, D.R., 2015.
579 Elemental ratio measurements of organic compounds using aerosol mass spectrometry:
580 characterization, improved calibration, and implications. Atmospheric Chemistry and Physics 15, 253-
581 272.
582 Cappa, C.D., Wilson, K.R., 2012. Multi-generation gas-phase oxidation, equilibrium partitioning, and
583 the formation and evolution of secondary organic aerosol. Atmospheric Chemistry and Physics 12,
584 9505-9528.
585 Chandrasekaran, S.R., Hopke, P.K., Newtown, M., Hurlbut, A., 2013. Residential-scale biomass boiler
586 emissions and efficiency characterization for several fuels. Energy and Fuels 27, 4840-4849.
587 Cocchi, M., 2011. Global Wood Pellet Industry Market and Trade Study. IEA Bioenergy.
588 Corbin, J.C., Keller, A., Lohmann, U., Burtscher, H., Sierau, B., Mensah, A.A., 2015. Organic Emissions
589 from a Wood Stove and a Pellet Stove before and after Simulated Atmospheric Aging. Aerosol
590 Science and Technology 49, 1037-1050.
591 Czech, H., Sippula, O., Kortelainen, M., Tissari, J., Radischat, C., Passig, J., Streibel, T., Jokiniemi, J.,
592 Zimmermann, R., 2016. On-line analysis of organic emissions from residential wood combustion with
593 single-photon ionisation time-of-flight mass spectrometry (SPI-TOFMS). Fuel 177, 334-342.
594 Ehhalt, D.H., 1999. Photooxidation of trace gases in the troposphere. Physical Chemistry Chemical
595 Physics 1, 5401-5408.
596 Elsasser, M., Crippa, M., Orasche, J., Decarlo, P.F., Oster, M., Pitz, M., Cyrys, J., Gustafson, T.L.,
597 Pettersson, J.B.C., Schnelle-Kreis, J., Prévôt, A.S.H., Zimmermann, R., 2012. Organic molecular
598 markers and signature from wood combustion particles in winter ambient aerosols: Aerosol mass
599 spectrometer (AMS) and high time-resolved GC-MS measurements in Augsburg, Germany.
600 Atmospheric Chemistry and Physics 12, 6113-6128.
601 Eriksson, A.C., Nordin, E.Z., Nyström, R., Pettersson, E., Swietlicki, E., Bergvall, C., Westerholm, R.,
602 Boman, C., Pagels, J.H., 2014. Particulate PAH emissions from residential biomass combustion: Time-
603 resolved analysis with aerosol mass spectrometry. Environmental Science and Technology 48, 7143-
604 7150.
605 Ervens, B., Carlton, A.G., Turpin, B.J., Altieri, K.E., Kreidenweis, S.M., Feingold, G., 2008. Secondary
606 organic aerosol yields from cloud-processing of isoprene oxidation products. Geophysical Research
607 Letters 35.

608 Evtyugina, M., Alves, C., Calvo, A., Nunes, T., Tarelho, L., Duarte, M., Prozil, S.O., Evtuguin, D.V., Pio,
609 C., 2014. VOC emissions from residential combustion of Southern and mid-European woods.
610 Atmospheric Environment 83, 90-98.
611 Garcia-Maraver, A., Zamorano, M., Fernandes, U., Rabaçal, M., Costa, M., 2014. Relationship
612 between fuel quality and gaseous and particulate matter emissions in a domestic pellet-fired boiler.
613 Fuel 119, 141-152.
614 Grieshop, A.P., Logue, J.M., Donahue, N.M., Robinson, A.L., 2009. Laboratory investigation of
615 photochemical oxidation of organic aerosol from wood fires 1: Measurement and simulation of
616 organic aerosol evolution. Atmospheric Chemistry and Physics 9, 1263-1277.
617 Hanley, L., Zimmermann, R., 2009. Light and molecular ions: The emergence of vacuum UV single-
618 photon ionization in MS. Analytical Chemistry 81, 4174-4182.
619 Heald, C.L., Kroll, J.H., Jimenez, J.L., Docherty, K.S., Decarlo, P.F., Aiken, A.C., Chen, Q., Martin, S.T.,
620 Farmer, D.K., Artaxo, P., 2010. A simplified description of the evolution of organic aerosol
621 composition in the atmosphere. Geophysical Research Letters 37.
622 Hennigan, C.J., Miracolo, M.A., Engelhart, G.J., May, A.A., Presto, A.A., Lee, T., Sullivan, A.P.,
623 McMeeking, G.R., Coe, H., Wold, C.E., Hao, W.M., Gilman, J.B., Kuster, W.C., De Gouw, J., Schichtel,
624 B.A., Collett Jr, J.L., Kreidenweis, S.M., Robinson, A.L., 2011. Chemical and physical transformations of
625 organic aerosol from the photo-oxidation of open biomass burning emissions in an environmental
626 chamber. Atmospheric Chemistry and Physics 11, 7669-7686.
627 Heringa, M.F., DeCarlo, P.F., Chirico, R., Lauber, A., Doberer, A., Good, J., Nussbaumer, T., Keller, A.,
628 Burtscher, H., Richard, A., Miljevic, B., Prevot, A.S.H., Baltensperger, U., 2012. Time-resolved
629 characterization of primary emissions from residential wood combustion appliances. Environmental
630 Science and Technology 46, 11418-11425.
631 Heringa, M.F., DeCarlo, P.F., Chirico, R., Tritscher, T., Dommen, J., Weingartner, E., Richter, R.,
632 Wehrle, G., Prévôt, A.S.H., Baltensperger, U., 2011. Investigations of primary and secondary
633 particulate matter of different wood combustion appliances with a high-resolution time-of-flight
634 aerosol mass spectrometer. Atmospheric Chemistry and Physics 11, 5945-5957.
635 Huang, R.J., Zhang, Y., Bozzetti, C., Ho, K.F., Cao, J.J., Han, Y., Daellenbach, K.R., Slowik, J.G., Platt,
636 S.M., Canonaco, F., Zotter, P., Wolf, R., Pieber, S.M., Bruns, E.A., Crippa, M., Ciarelli, G., Piazzalunga,
637 A., Schwikowski, M., Abbaszade, G., Schnelle-Kreis, J., Zimmermann, R., An, Z., Szidat, S.,
638 Baltensperger, U., El Haddad, I., Prévôt, A.S.H., 2015. High secondary aerosol contribution to
639 particulate pollution during haze events in China. Nature 514, 218-222.
640 Jalava, P.I., Happo, M.S., Kelz, J., Brunner, T., Hakulinen, P., Mäki-Paakkanen, J., Hukkanen, A.,
641 Jokiniemi, J., Obernberger, I., Hirvonen, M.R., 2012. Invitro toxicological characterization of

642 particulate emissions from residential biomass heating systems based on old and new technologies.
643 Atmospheric Environment 50, 24-35.
644 Jimenez, J.L., Jayne, J.T., Shi, Q., Kolb, C.E., Worsnop, D.R., Yourshaw, I., Seinfeld, J.H., Flagan, R.C.,
645 Zhang, X., Smith, K.A., Morris, J.W., Davidovits, P., 2003. Ambient aerosol sampling using the
646 Aerodyne aerosol mass spectrometer. Journal of Geophysical Research D: Atmospheres 108, SOS 13-
647 11 SOS 13-13.
648 Johansson, L.S., Leckner, B., Gustavsson, L., Cooper, D., Tullin, C., Potter, A., 2004. Emission
649 characteristics of modern and old-type residential boilers fired with wood logs and wood pellets.
650 Atmospheric Environment 38, 4183-4195.
651 Kaivosoja, T., Jalava, P.I., Lamberg, H., Virén, A., Tapanainen, M., Torvela, T., Tapper, U., Sippula, O.,
652 Tissari, J., Hillamo, R., Hirvonen, M.R., Jokiniemi, J., 2013. Comparison of emissions and toxicological
653 properties of fine particles from wood and oil boilers in small (20-25kW) and medium (5-10MW)
654 scale. Atmospheric Environment 77, 193-201.
655 Kang, E., Root, M.J., Toohey, D.W., Brune, W.H., 2007. Introducing the concept of Potential Aerosol
656 Mass (PAM). Atmospheric Chemistry and Physics 7, 5727-5744.
657 Kari, E., Hao, L., Yli-Pirilä, P., Leskinen, A., Kortelainen, M., Grigonyte, J., Worsnop, D.R., Jokiniemi, J.,
658 Sippula, O., Faiola, C.L., Virtanen, A., 2017. Effect of Pellet Boiler Exhaust on Secondary Organic
659 Aerosol Formation from α-Pinene. Environmental Science and Technology 51, 1423-1432.
660 Keller, A., Burtscher, H., 2012. A continuous photo-oxidation flow reactor for a defined measurement
661 of the SOA formation potential of wood burning emissions. Journal of Aerosol Science 49, 9-20.
662 Kinsey, J.S., Touati, A., Yelverton, T.L.B., Aurell, J., Cho, S.H., Linak, W.P., Gullett, B.K., 2012. Emissions
663 characterization of residential wood-fired hydronic heater technologies. Atmospheric Environment
664 63, 239-249.
665 Kroll, J.H., Donahue, N.M., Jimenez, J.L., Kessler, S.H., Canagaratna, M.R., Wilson, K.R., Altieri, K.E.,
666 Mazzoleni, L.R., Wozniak, A.S., Bluhm, H., Mysak, E.R., Smith, J.D., Kolb, C.E., Worsnop, D.R., 2011.
667 Carbon oxidation state as a metric for describing the chemistry of atmospheric organic aerosol.
668 Nature Chemistry 3, 133-139.
669 Krutul, D., Zielenkiewicz, T., Antczak, A., Zawadzki, J., Radomski, A., Kupczyk, M., Drozdzek, M., 2011.
670 Influence of the environmental pollution on the chemical composition of bark and wood of trunk,
671 branches and main roots of birch (Betula pendula Roth.). Annals of Warsaw University of Life
672 Sciences (SGGW): Forestry and Wood Technology 74, 242-248.
673 Künzi, L., Mertes, P., Schneider, S., Jeannet, N., Menzi, C., Dommen, J., Baltensperger, U., Prévôt,
674 A.S.H., Salathe, M., Kalberer, M., Geiser, M., 2013. Responses of lung cells to realistic exposure of
675 primary and aged carbonaceous aerosols. Atmospheric Environment 68, 143-150.

676 Lambe, A.T., Ahern, A.T., Williams, L.R., Slowik, J.G., Wong, J.P.S., Abbatt, J.P.D., Brune, W.H., Ng,
677 N.L., Wright, J.P., Croasdale, D.R., Worsnop, D.R., Davidovits, P., Onasch, T.B., 2011. Characterization
678 of aerosol photooxidation flow reactors: Heterogeneous oxidation, secondary organic aerosol
679 formation and cloud condensation nuclei activity measurements. Atmospheric Measurement
680 Techniques 4, 445-461.
681 Lamberg, H., Nuutinen, K., Tissari, J., Ruusunen, J., Yli-Pirilä, P., Sippula, O., Tapanainen, M., Jalava, P.,
682 Makkonen, U., Teiniä, K., Saarnio, K., Hillamo, R., Hirvonen, M.R., Jokiniemi, J., 2011a.
683 Physicochemical characterization of fine particles from small-scale wood combustion. Atmospheric
684 Environment 45, 7635-7643.
685 Lamberg, H., Sippula, O., Tissari, J., Jokiniemi, J., 2011b. Effects of air staging and load on fine-particle
686 and gaseous emissions from a small-scale pellet boiler. Energy and Fuels 25, 4952-4960.
687 Li, R., Palm, B.B., Ortega, A.M., Hlywiak, J., Hu, W., Peng, Z., Day, D.A., Knote, C., Brune, W.H., De
688 Gouw, J.A., Jimenez, J.L., 2015. Modeling the radical chemistry in an oxidation flow reactor: Radical
689 formation and recycling, sensitivities, and the OH exposure estimation equation. Journal of Physical
690 Chemistry A 119, 4418-4432.
691 Liu, P.S.K., Deng, R., Smith, K.A., Williams, L.R., Jayne, J.T., Canagaratna, M.R., Moore, K., Onasch,
692 T.B., Worsnop, D.R., Deshler, T., 2007. Transmission efficiency of an aerodynamic focusing lens
693 system: Comparison of model calculations and laboratory measurements for the aerodyne aerosol
694 mass spectrometer. Aerosol Science and Technology 41, 721-733.
695 Madlener, R., Koller, M., 2007. Economic and CO2 mitigation impacts of promoting biomass heating
696 systems: An input-output study for Vorarlberg, Austria. Energy Policy 35, 6021-6035.
697 Martinsson, J., Eriksson, A.C., Nielsen, I.E., Malmborg, V.B., Ahlberg, E., Andersen, C., Lindgren, R.,
698 Nyström, R., Nordin, E.Z., Brune, W.H., Svenningsson, B., Swietlicki, E., Boman, C., Pagels, J.H., 2015.
699 Impacts of Combustion Conditions and Photochemical Processing on the Light Absorption of Biomass
700 Combustion Aerosol. Environmental Science and Technology 49, 14663-14671.
701 Miljevic, B., Heringa, M.F., Keller, A., Meyer, N.K., Good, J., Lauber, A., Decarlo, P.F., Fairfull-Smith,
702 K.E., Nussbaumer, T., Burtscher, H., Prévôt, A.S.H., Baltensperger, U., Bottle, S.E., Ristovski, Z.D.,
703 2010. Oxidative potential of logwood and pellet burning particles assessed by a novel profluorescent
704 nitroxide probe. Environmental Science and Technology 44, 6601-6607.
705 Mülhopt, S., Dilger, M., Diabaté, S., Schlager, C., Krebs, T., Zimmermann, R., Buters, J., Oeder, S.,
706 Wäscher, T., Weiss, C., Paur, H.R., 2016. Toxicity testing of combustion aerosols at the air-liquid
707 interface with a self-contained and easy-to-use exposure system. Journal of Aerosol Science 96, 38-
708 55.

709 Ng, N.L., Canagaratna, M.R., Jimenez, J.L., Chhabra, P.S., Seinfeld, J.H., Worsnop, D.R., 2011. Changes
710 in organic aerosol composition with aging inferred from aerosol mass spectra. Atmospheric
711 Chemistry and Physics 11, 6465-6474.
712 Ng, N.L., Canagaratna, M.R., Zhang, Q., Jimenez, J.L., Tian, J., Ulbrich, I.M., Kroll, J.H., Docherty, K.S.,
713 Chhabra, P.S., Bahreini, R., Murphy, S.M., Seinfeld, J.H., Hildebrandt, L., Donahue, N.M., Decarlo, P.F.,
714 Lanz, V.A., Prévôt, A.S.H., Dinar, E., Rudich, Y., Worsnop, D.R., 2010. Organic aerosol components
715 observed in Northern Hemispheric datasets from Aerosol Mass Spectrometry. Atmospheric
716 Chemistry and Physics 10, 4625-4641.
717 Ng, N.L., Kroll, J.H., Keywood, M.D., Bahreini, R., Varutbangkul, V., Flagan, R.C., Seinfeld, J.H., Lee, A.,
718 Goldstein, A.H., 2006. Contribution of first- versus second-generation products to secondary organic
719 aerosols formed in the oxidation of biogenic hydrocarbons. Environmental Science and Technology
720 40, 2283-2297.
721 Nordin, E.Z., Uski, O., Nyström, R., Jalava, P., Eriksson, A.C., Genberg, J., Roldin, P., Bergvall, C.,
722 Westerholm, R., Jokiniemi, J., Pagels, J.H., Boman, C., Hirvonen, M.R., 2015. Influence of ozone
723 initiated processing on the toxicity of aerosol particles from small scale wood combustion.
724 Atmospheric Environment 102, 282-289.
725 Obaidullah, M., Bram, S., Verma, V.K., De Ruyck, J., 2012. A review on particle emissions from small
726 scale biomass combustion. International Journal of Renewable Energy Research 2, 147-159.
727 Olsson, M., Kjällstrand, J., Petersson, G., 2003. Specific chimney emissions and biofuel characteristics
728 of softwood pellets for residential heating in Sweden. Biomass and Bioenergy 24, 51-57.
729 Onasch, T.B., Trimborn, A., Fortner, E.C., Jayne, J.T., Kok, G.L., Williams, L.R., Davidovits, P., Worsnop,
730 D.R., 2012. Soot particle aerosol mass spectrometer: Development, validation, and initial application.
731 Aerosol Science and Technology 46, 804-817.
732 Orasche, J., Seidel, T., Hartmann, H., Schnelle-Kreis, J., Chow, J.C., Ruppert, H., Zimmermann, R.,
733 2012. Comparison of emissions from wood combustion. part 1: Emission factors and characteristics
734 from different small-scale residential heating appliances considering particulate matter and
735 polycyclic aromatic hydrocarbon (PAH)-related toxicological potential of particle-bound organic
736 species. Energy and Fuels 26, 6695-6704.
737 Ortega, A.M., Day, D.A., Cubison, M.J., Brune, W.H., Bon, D., De Gouw, J.A., Jimenez, J.L., 2013.
738 Secondary organic aerosol formation and primary organic aerosol oxidation from biomass-burning
739 smoke in a flow reactor during FLAME-3. Atmospheric Chemistry and Physics 13, 11551-11571.
740 Ozgen, S., Caserini, S., Galante, S., Giugliano, M., Angelino, E., Marongiu, A., Hugony, F., Migliavacca,
741 G., Morreale, C., 2014. Emission factors from small scale appliances burning wood and pellets.
742 Atmospheric Environment 94, 144-153.

743 Pieber, S.M., El Haddad, I., Slowik, J.G., Canagaratna, M.R., Jayne, J.T., Platt, S.M., Bozzetti, C.,
744 Daellenbach, K.R., Fröhlich, R., Vlachou, A., Klein, F., Dommen, J., Miljevic, B., Jiménez, J.L., Worsnop,
745 D.R., Baltensperger, U., Prévôt, A.S.H., 2016. Inorganic Salt Interference on CO2 + in Aerodyne AMS
746 and ACSM Organic Aerosol Composition Studies. Environmental Science and Technology 50, 10494-
747 10503.
748 Reda, A.A., Czech, H., Schnelle-Kreis, J., Sippula, O., Orasche, J., Weggler, B., Abbaszade, G., Arteaga-
749 Salas, J.M., Kortelainen, M., Tissari, J., Jokiniemi, J., Streibel, T., Zimmermann, R., 2015. Analysis of
750 gas phase carbonyl compounds in emissions from modern wood combustion appliances: influence of
751 wood type and combustion appliance. Energy and Fuels 29, 3897-3907.
752 Riva, M., Robinson, E.S., Perraudin, E., Donahue, N.M., Villenave, E., 2015. Photochemical aging of
753 secondary organic aerosols generated from the photooxidation of polycyclic aromatic hydrocarbons
754 in the gas-phase. Environmental Science and Technology 49, 5407-5416.
755 Sehlstedt, M., Dove, R., Boman, C., Pagels, J., Swietlicki, E., Löndahl, J., Westerholm, R., Bosson, J.,
756 Barath, S., Behndig, A.F., Pourazar, J., Sandström, T., Mudway, I.S., Blomberg, A., 2010. Antioxidant
757 airway responses following experimental exposure to wood smoke in man. Particle and Fibre
758 Toxicology 7.
759 Sippula, O., Hytönen, K., Tissari, J., Raunemaa, T., Jokiniemi, J., 2007. Effect of wood fuel on the
760 emissions from a top-feed pellet stove. Energy and Fuels 21, 1151-1160.
761 Stephens, M., Turner, N., Sandberg, J., 2003. Particle identification by laser-induced incandescence in
762 a solid-state laser cavity. Applied Optics 42, 3726-3736.
763 Stockwell, C.E., Yokelson, R.J., Kreidenweis, S.M., Robinson, A.L., Demott, P.J., Sullivan, R.C., Reardon,
764 J., Ryan, K.C., Griffith, D.W.T., Stevens, L., 2014. Trace gas emissions from combustion of peat, crop
765 residue, domestic biofuels, grasses, and other fuels: Configuration and Fourier transform infrared
766 (FTIR) component of the fourth Fire Lab at Missoula Experiment (FLAME-4). Atmospheric Chemistry
767 and Physics 14, 9727-9754.
768 Tiitta, P., Leskinen, A., Hao, L., Yli-Pirilä, P., Kortelainen, M., Grigonyte, J., Tissari, J., Lamberg, H.,
769 Hartikainen, A., Kuuspalo, K., Kortelainen, A., Virtanen, A., Lehtinen, K.E.J., Komppula, M., Pieber, S.,
770 Prévôt, A.S.H., Onasch, T.B., Worsnop, D.R., Czech, H., Zimmermann, R., Jokiniemi, J., Sippula, O.,
771 2016. Transformation of logwood combustion emissions in a smog chamber: formation of secondary
772 organic aerosol and changes in the primary organic aerosol upon daytime and nighttime aging.
773 Atmospheric Chemistry and Physics 16, 13251-13269.
774 Tkacik, D.S., Lambe, A.T., Jathar, S., Li, X., Presto, A.A., Zhao, Y., Blake, D., Meinardi, S., Jayne, J.T.,
775 Croteau, P.L., Robinson, A.L., 2014. Secondary organic aerosol formation from in-use motor vehicle
776 emissions using a potential aerosol mass reactor. Environmental Science and Technology 48, 11235-
777 11242.

778 Trivitayanurak, W., Adams, P.J., 2014. Does the POA-SOA split matter for global CCN formation?
779 Atmospheric Chemistry and Physics 14, 995-1010.
780 Venturini, E., Vassura, I., Zanetti, C., Pizzi, A., Toscano, G., Passarini, F., 2015. Evaluation of non-
781 steady state condition contribution to the total emissions of residential wood pellet stove. Energy 88,
782 650-657.
783 Verma, V.K., Bram, S., Gauthier, G., De Ruyck, J., 2011. Performance of a domestic pellet boiler as a
784 function of operational loads: Part-2. Biomass and Bioenergy 35, 272-279.
785 Vicente, E.D., Duarte, M.A., Tarelho, L.A.C., Nunes, T.F., Amato, F., Querol, X., Colombi, C., Gianelle,
786 V., Alves, C.A., 2015. Particulate and gaseous emissions from the combustion of different biofuels in a
787 pellet stove. Atmospheric Environment 120, 15-27.
788 Win, K.M., Persson, T., Bales, C., 2012. Particles and gaseous emissions from realistic operation of
789 residential wood pellet heating systems. Atmospheric Environment 59, 320-327.
790 Wu, R., Pan, S., Li, Y., Wang, L., 2014. Atmospheric oxidation mechanism of toluene. Journal of
791 Physical Chemistry A 118, 4533-4547.
792
793
794

795 **Fig. 1.** Averaged SPI mass spectra of organic vapours for the four investigated operation
796 conditions of softwood pellets (a) boiler start phase (BSP), (b) optimal combustion (OPT), (c)
797 reduced secondary air supply (RSA) and (d) optimal combustion of birch bark pellets (BBP).
798 The concentration of the internal standard (IS, D_3-toluene) was constant for all experiment
799 and appears with its molecular ion at m/z 95 (bold).

800

Fig. 2. Temporal evolution of concentrations (O_2 and CO_2), EFs (NO_x, CO, benzene (BENZ), acetaldehyde (AA) and butadiene (BTD)) and modified combustion efficiency over boiler start phase (BSP), optimised combustion (OPT), combustion with reduced secondary air (RSA) of softwood pellets as well as optimised combustion of birch bark pellets (BBP).

Fig. 3. Van Krevelen diagram of aged (red) and non-aged OA (blue) from combustion conditions OPT (circles) and RSA (squares). Solid purple lines belong to slopes from (Heald et al., 2010) which indicate main functionalisation of OA, where the black lines represent slopes from non-aged to aged OA (-0.44±0.07 for OPT and -0.47±0.10 for RSA). The grey area refers to the triangular space of f_{44} vs. f_{43} in which ambient OA was found to be usually located (Ng et al., 2010), converted into the H:C vs. O:C dimension. Dashed lines are average carbon oxidation states (OSC) (Kroll et al., 2011).

814 **Fig. 4.** Relative compound class distribution for OPT (circles) and RSA (squares) with
815 standard deviations. Data points below the diagonal line show relative increase in the organic
816 fraction after ageing (ER > 1), whereas data points above the diagonal lines show decrease
817 in relative organic fraction (ER < 1).

818

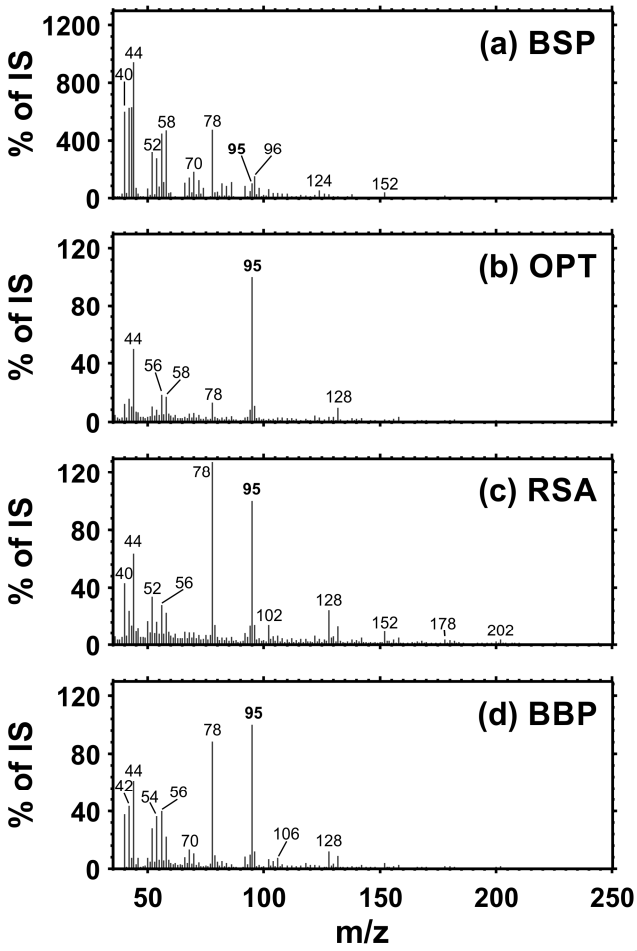

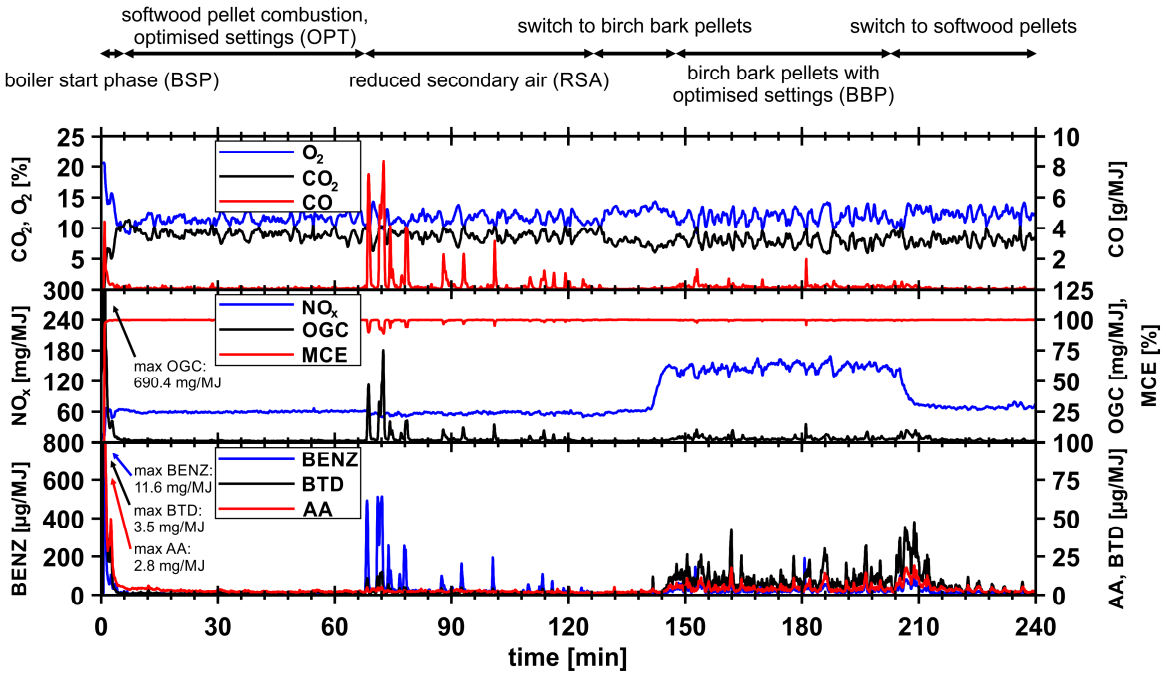

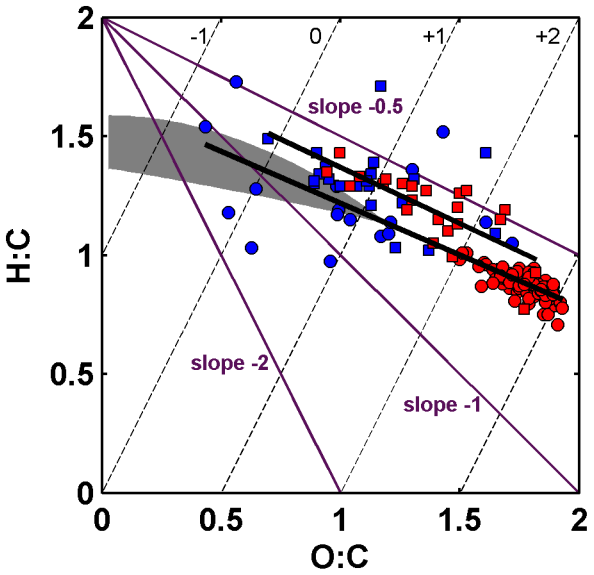

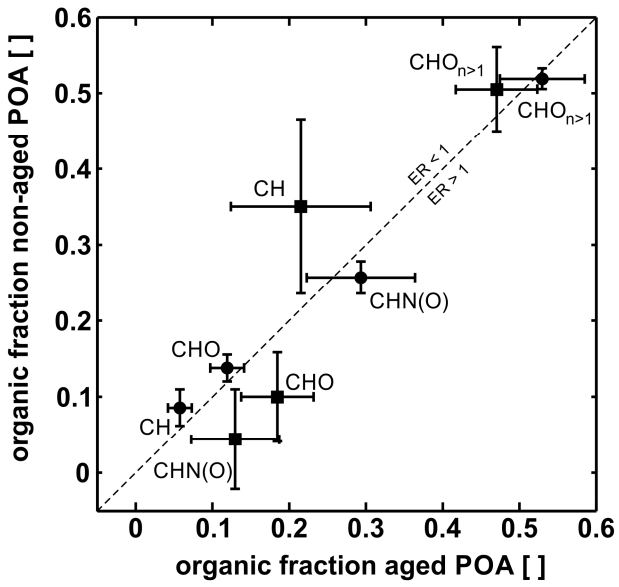

Highlights:

- composition of VOC emissions from pellet boiler at different combustion conditions
- very low concentrations of wood-related VOCs in primary emissions
- low primary emissions accompany low secondary SOA formation potential
- total SOA yield measured with PAM and estimated from precursor yields